J. Fluid Mech. (1995), vol. 303, pp. 155–167

The structure of highly sheared turbulence

By F. A. DE SOUZA[1]†, V. D. NGUYEN[2] AND S. TAVOULARIS[1]

[1]Department of Mechanical Engineering, University of Ottawa, Ottawa, Ontario K1N 6N5, Canada
[2]High Speed Aerodynamics Laboratory, National Research Council of Canada, Ottawa, Ontario K1A 0R6, Canada

(Received 20 September 1994 and in revised form 5 June 1995)

Uniformly sheared flows have been generated in a high-speed wind tunnel at shear rates higher than previously achieved, in an effort to approach those in the inner turbulent boundary layer. As at lower shear rates, the turbulence structure was found to attain a self-similar state with approximately constant anisotropies and exponential kinetic energy growth. The normal Reynolds stress anisotropies showed no systematic dependence upon the mean shear within the examined range; however, the shear stress anisotropy was significantly lower than the low-shear values, in conformity with boundary layer measurements and direct numerical simulations of homogeneous shear flow.

1. Introduction

In any turbulent shear flow, both the mean velocity distribution and the structure of turbulence depend strongly upon the boundary conditions, including the inflow and outflow conditions to the considered control volume. In general, flows in different geometrical configurations develop different mean and turbulent fields and, even in relatively simple geometries, there can be local or temporal variations of the type of prevalent eddy structures, reflecting variations in the shape of the boundary or in the incoming flow. In particular, it has been well accepted that, in a turbulent boundary layer, the dominant turbulence structure near the wall is a set of elongated, counter-rotating, quasi-streamwise vortices, quite distinct from the 'hairpin vortex' type of dominant structure encountered away from the wall. Although, undoubtedly, this structural difference is caused by the wall, it has not yet been clarified whether the near-wall structure is mainly a kinematic effect of wall proximity (no-penetration) or it is due to the fact that mean shear attains its highest values near the wall, where viscous actions are increased (no-slip). Mean shear, irrespectively of its origin, generates turbulence and actively interacts with it; thus, it seems instructive to investigate shearing effects without the additional complications introduced by a solid boundary.

The simplest type of turbulent shear flow would be an unbounded, uniformly sheared flow (USF), in which turbulence would be homogeneous. In such a configuration, and at sufficiently large Reynolds number, one may anticipate that turbulence statistics, properly non-dimensionalized, would be universal, namely independent of

† Present address: Centre d'Etudes Aérodynamiques et Thermiques, Université de Poitiers, 43 Rue de l'Aérodrome, 86036 Poitiers CEDEX, France.

the value of the mean shear. Uniformly sheared flows have been studied, in approximate forms, both experimentally, in wind tunnels, as well as analytically, by direct numerical simulation (DNS). Most studies have generally concluded that the structure of such flows resembles fairly closely the structure of the outer region of turbulent boundary layers, to the extent that even 'hairpin vortices' have been identified numerically (Rogers & Moin 1987). However, a recent DNS of homogeneous flow at high shear rates (Lee, Kim & Moin 1990) revealed the presence of streaky vortices and a turbulence structure similar to those observed in the inner boundary layer. As the effective shear rate increased, these vortices became increasingly elongated in the flow direction and narrow in the spanwise direction. Most recently, Brereton & Hwang (1994) correlated the spanwise streak spacing with the total distortion of large eddies by the mean shear, in an attempt to reconcile the average non-dimensionalized streak spacing measured in steady wall-bounded flows with that in unbounded homogeneous turbulent flow at high shear rate. These studies have introduced the possibility that differences in mean shear magnitude, even in the absence of a solid boundary, may be responsible for at least some of the structural differences among turbulent shear flows. They also support the plausibility that the very near-wall structure, whose experimental documentation is often difficult, can be reproduced in USF at very high shear rate. Previous USF experiments have been limited to modest shear rates, up to 84 s^{-1} (Tavoularis & Karnik 1989, hereafter referred to as TK), whereas in a moderate Reynolds number viscous sublayer the shear rate is more likely to exceed 500 s^{-1}. This prompts the present study, whose primary objectives are to generate USF at shear rates higher than those in earlier studies and, if possible, comparable to values in the inner region of a turbulent boundary layer. Turbulence measurements in these flows will be compared with near-wall data from the literature and with the high-shear DNS, in an effort to identify the causes of the structural peculiarities of turbulent eddies very close to the wall, where it is believed that most of the turbulence production originates. A long-term goal of studies such as the present one is to understand fully the factors that determine the structure of any turbulent shear flow.

2. Experimental facilities and procedures

All experiments were conducted in the 127 × 127 mm pilot wind tunnel at the High Speed Aerodynamics Laboratory of the National Research Council's Institute of Aerospace Research, in Ottawa, Canada. This facility is a pressurized, blowdown, wind tunnel, capable of running in the subsonic, transonic and supersonic flow regimes. It was supplied with compressed air at up to about 2.1 MPa from storage tanks with a capacity of 1430 m^3, which provided the means for continuous running. The air temperature in the settling chamber was stabilized via thermal matrices to a typical level of about 21°C. An automatic pressure control valve maintained the settling chamber pressure constant at the pre-selected value of 165 kPa. From the settling chamber, the air passed through a number of turbulence reduction screens, a nozzle with a contraction ratio 10:1 and the test section, before exhausting to the atmosphere via a variable-geometry supersonic/subsonic diffuser, which is a two-dimensional duct with fixed top and bottom walls and articulated sidewalls. A schematic drawing of the facility is shown in figure 1.

The shear generator was housed in a sturdy aluminium frame, bolted between the contraction section and the test section. A flow separator module, made of nine 0.792 mm stainless steel plates, was inserted into the frame to divide the flow into ten, 12.7 mm high, parallel channels. The blockage necessary for generating shear was

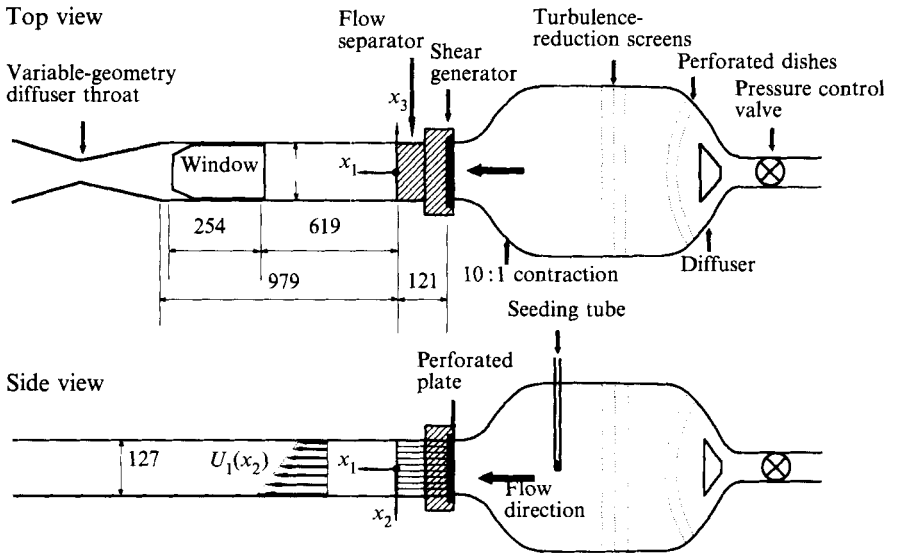

FIGURE 1. Schematic drawing of the flow facility; all dimensions in mm.

created by a 3.2 mm thick, perforated, aluminium plate, inserted in the aluminium frame immediately upstream of the flow separator. Three different perforated plates were manufactured, each with ten 12.7 mm high rows of varying solidity. To ensure transverse uniformity of scales and to further straighten the flow, the separator channels extended downstream by 121 mm. A variety of USFs could be generated by changing the perforated plate and by adjusting the flow rate of the tunnel.

Mean velocity and turbulence measurements were conducted via a frequency-shifted, two-component, fibre optic, laser-Doppler velocimeter (LDV), employing a 100 mW Argon–Ion laser and operating in the backscatter mode. The ellipsoidal measurement volume had a height (transverse to the flow direction) of about 1.2 mm and a diameter of about 0.1 mm. Optical access to the flow was provided by a glass window, 254 mm long and 127 mm wide. The LDV probe head was mounted on a three-dimensional manual traversing table over the glass window. The test section floor was painted black in order to minimize reflection of the incident laser beams. The flow was seeded with fine propylene glycol droplets of roughly 0.6 μm in diameter, generated by a six-jet atomizer (TSI model 9306), which was supplied with compressed air at 620 kPa. The seeding particles were introduced on the centreline axis of the settling chamber immediately upstream of the contraction section via a 17.5 mm ID aluminium tube. The DANTEC FLOware software, run on a microcomputer, was used for all LDV data acquisition and much of the initial data processing. A number of computer programs were written for further processing and calculation of turbulence statistics.

The LDV system could measure simultaneously only the two components of velocity which were normal to the axis of the optical probe. In the absence of windows on the test section's sidewalls, it was not possible to measure the vertical velocity component, which for the usual shear generator orientation was parallel to the mean shear direction. This component was measured after rotating the shear generator by 90°. As a verification that the flow properties were not changed by this action, it was ensured that the statistics of the streamwise component, measured with the shear generator in both orientations, were essentially the same.

Case	$\overline{U}_c$ (m s^{-1})	$d\overline{U}_1/dx_2$ (s^{-1})	k_s (m^{-1})	m_{11}	m_{22}	m_{33}	$-m_{12}$	$-\rho$
1	35.1	436	12.4	0.16	−0.13	−0.03	0.093	0.30
2	34.1	665	19.5	0.20	−0.14	−0.06	0.105	0.36
3	44.6	705	15.8	0.13	−0.10	−0.03	0.106	0.33
4	38.8	705	18.2	0.21	−0.13	−0.08	0.121	0.36
5	54.7	646	11.8	0.10	−0.10	−0.00	0.109	0.34
6	35.2	646	18.3	0.21	−0.13	−0.08	0.120	0.38
TC	12.4	47	3.8	0.20	−0.14	−0.06	0.140	0.44
TK	13.0	84	6.6	0.22	−0.13	−0.09	0.165	0.50

Case	κ	ϵ/P	t_u/t_s	τ_r	Δh (mm)	$L_{11,1r}/\Delta h$	$\lambda_{11r}/\Delta h$	$\eta_r/\Delta h$	$R_{\lambda 1}$
1	0.10	0.5	21.8	9.0	12.7	5.2	0.18	0.0026	1010
2	0.08	0.6	15.7	11.8	12.7	4.1	0.13	0.0017	1180
3	0.07	0.7	14.2	13.0	12.7	3.7	0.12	0.0016	1080
4	0.07	0.7	11.9	12.0	12.7	3.0	0.11	0.0015	1050
5	0.11	0.5	18.0	9.9	12.7	4.5	0.14	0.0019	1080
6	0.07	0.7	11.7	14.6	12.7	3.4	0.11	0.0016	1120
TC	0.12	0.6	12.5	11.6	30.8	1.7	0.18	0.0062	245
TK	0.09	0.7	8.6	20.1	25.4	1.5	0.19	0.0053	310

TABLE 1. Summary of measured and estimated parameters in the present and some previous USFs; TC, Tavoularis & Corrsin (1981); TK, Tavoularis & Karnik (1989)

Because the main conclusions of this study depend entirely on the accuracy of turbulence measurements, particularly that of the shear stress, substantial effort was made to identify all possible sources of error and to estimate appropriate corrections, sometimes under the assumption of extremely adverse conditions. The level of such corrections was low enough for the results to be judged as reliable. Details of the error analysis can be found in the thesis of the first author (de Souza 1993).

3. Measurements

3.1. *Flow uniformity and transverse homogeneity*

With all obstructions removed, the transverse and spanwise variations of the mean velocity components were within 2% of the centreline mean (interest was focused on the 'core', $-0.25 < x_2/h, x_3/h < 0.25$; $h = 127$ mm is the test section height). The r.m.s. turbulence intensity in the unobstructed tunnel, including all measurement uncertainties, was about 5% for the streamwise component and about 3% for the transverse and spanwise components. The shear stress correlation coefficient had a near-zero average and fluctuated randomly in the range between −0.10 and 0.10. Six different USFs were studied using the three perforated plates and different blockages of the end channels. Their main characteristics are summarized in table 1. Transverse shear flow profiles revealed mean velocity gradients which were uniform across most of the test section height and remained essentially constant along the streamwise extent of measurement (see figure 2 for a typical transverse profile of the streamwise mean velocity). The shear rates in the various flows ranged between 436 to 705 s^{-1}, and the shear generator constants, $k_s = (1/\overline{U}_c)(d\overline{U}_1/dx_2)$, between 11.8 and 19.5 m^{-1}. Typical maximum transverse inhomogeneities of the turbulent stresses in the core of the flow were about 20% in the transverse direction and 10% in the

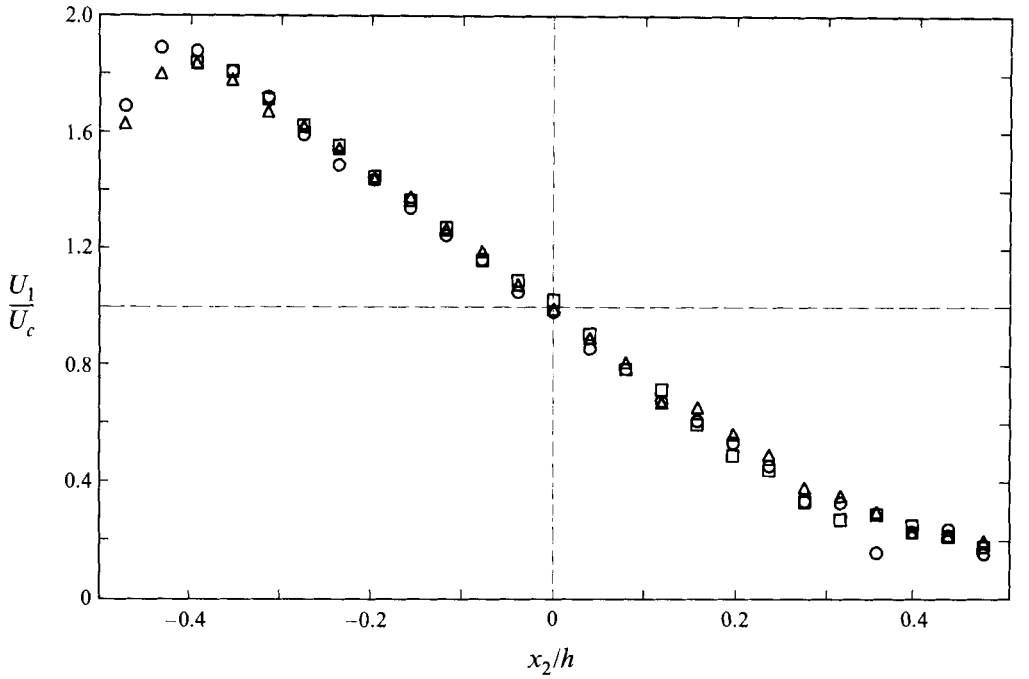

FIGURE 2. Example (case 4) of the transverse variation of the mean streamwise velocity: $x_1/h = 5.2$ (○), 6.0 (△) and 6.8 (□); $h = 127$ mm.

spanwise direction; this included both random and systematic variations. The shear stress correlation coefficient varied randomly by a maximum of 30% in the same region. In all cases, much of the uncertainty was due to scatter, which was reduced considerably by increasing the number of samples. For a comparison, it may be pointed out that inhomogeneities of the order of 15% are not uncommon, even in the best USF realizations (TK). In conclusion, the shear non-uniformity and turbulence inhomogeneity levels in the present flows could be judged as comparable to those in a reliable low-shear USF.

3.2. *Downstream development of turbulence*

The streamwise evolution of the four dominant Reynolds stresses and the turbulent kinetic energy per unit mass, $\frac{1}{2}q^2 = \frac{1}{2}(\overline{u_1^2} + \overline{u_2^2} + \overline{u_3^2})$, non-dimensionalized by the centreline velocity, $\overline{U}_c$, and plotted versus the logarithm of the total strain, $\tau = k_s x_1$ (see figure 3*a*, as an example), was compatible with exponential growth of the form $e^{\kappa\tau}$ (Tavoularis 1985), where κ is a dimensionless constant, and consistent with previous USF experiments. The Reynolds stresses were ordered as $\overline{u_1^2} > \overline{u_3^2} > \overline{u_2^2} > |\overline{u_1 u_2}|$, the same as in turbulent boundary layers and other flows with a fixed dominant shear direction.

Previous studies (Rohr *et al.* 1988; TK) have indicated that plots of the ratios $\overline{u_i u_j}/\overline{U}_c^2$, corresponding to the same shear generator but different $\overline{U}_c$, essentially collapse when plotted versus the total strain. The present data formed three visibly distinct groups, each corresponding to a unique value or a narrow range of the shear generator constant: $11.8 < k_s < 12.4, k_s = 15.8$ and $18.2 < k_s < 19.5$.

The least-squares-fitted values of the dimensionless exponential growth rate, κ, were compatible with past measurements (TK), and exhibited roughly the same degree of

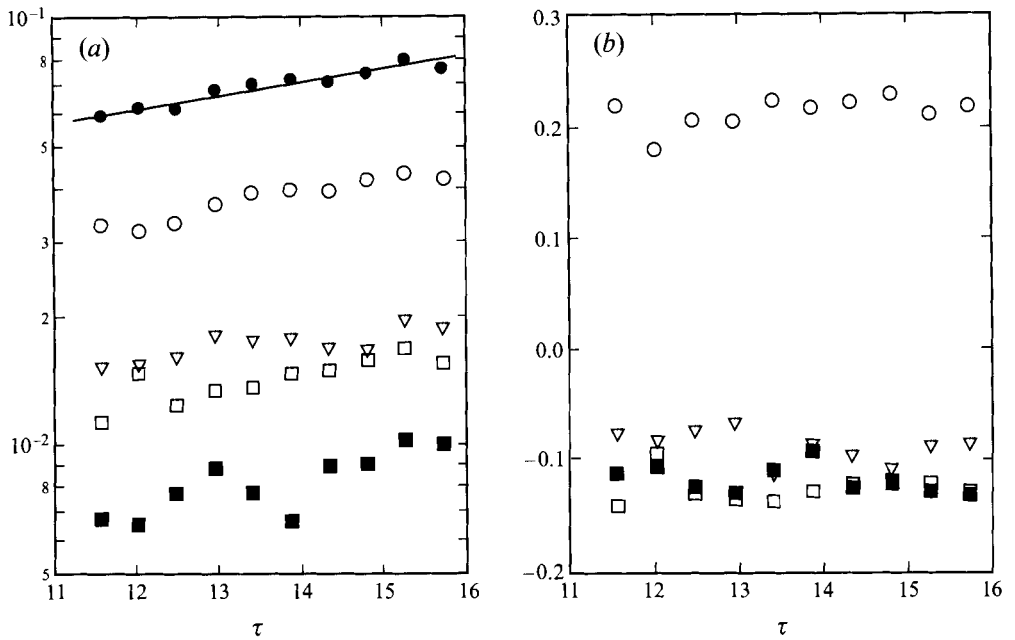

FIGURE 3. Example (case 4) of the streamwise evolution of (*a*) the dimensionless Reynolds stresses and turbulent kinetic energy (○, $\overline{u_1^2}/\overline{U_c}^2$; □, $\overline{u_2^2}/\overline{U_c}^2$; ▽, $\overline{u_3^2}/\overline{U_c}^2$; ■, $-\overline{u_1u_2}/\overline{U_c}^2$; •, $q^2/\overline{U_c}^2$) and (*b*) the Reynolds stress anisotropies (○, m_{11}; □, m_{22}; ▽, m_{33}; ■, $-m_{12}$).

scatter. The dimensionless growth rate, averaged over all of the present and several previous results, was $\kappa = 0.090$, with a standard deviation of 0.013. It is not clear whether an observed slight tendency of κ to decrease with increasing k_s is a real effect or due to scatter.

3.3. *The Reynolds stress tensor anisotropy*

In all USFs generated in the present study, the values of the Reynolds stress anisotropies,

$$m_{ij} = \frac{\overline{u_iu_j}}{q^2} - \tfrac{1}{3}\delta_{ij} \tag{3.1}$$

in the downstream half of the tunnel were practically constant (see figure 3*b*, for example). The level of anisotropy differed somewhat between flows with significantly different values of k_s, although it was not possible to identify systematic trends. The average over all present experiments was as follows:

$$m_{ij} = \begin{bmatrix} 0.18 \pm 0.04 & -0.11 \pm 0.01 & 0 \\ -0.11 \pm 0.01 & -0.12 \pm 0.02 & 0 \\ 0 & 0 & -0.05 \pm 0.03 \end{bmatrix}.$$

The diagonal components were in agreement with the average values of TK; however, the dominant shear term, $-m_{12}$, was consistently about 25% lower than the values between 0.14 and 0.16 reported in the USF literature. A decrease of similar magnitude was measured in the shear stress correlation coefficient, $\rho = \overline{u_1u_2}/(u'_1u'_2)$, relative to values in previous USF and outer boundary layers. The average value over all of the present flows was -0.35 ± 0.02, compared to previous values of between -0.40

and −0.50. The reductions in average $-m_{12}$ and ρ were measurably higher than any identifiable, systematic or random error (de Souza 1993).

3.4. *Estimates of lengthscales*

Owing to the relatively low data rate and insufficient spatial resolution of the LDV system, it was not possible to measure directly the various turbulence lengthscales. The best that could be done was to estimate these scales by using approximations established in previous USFs, in full awareness of the possible errors introduced by this procedure. These approximations require the dissipation rate, ϵ, of turbulent kinetic energy, which was estimated as the balance of the rates of production and convection of q^2.

The streamwise integral lengthscale of the streamwise velocity fluctuation, $L_{11,1}$, was estimated from the empirical expression

$$L_{11,1} = A\frac{q^3}{\epsilon} \tag{3.2}$$

with the value $A \approx 0.24$, adjusted to fit previous USF measurements. The above expression implies an exponential growth of the streamwise integral lengthscale, at exactly half the growth rate of the turbulent kinetic energy. Using this growth rate, nominal initial values were determined by extrapolating the $L_{11,1}$ estimates upstream to the exit of the shear generator. Such nominal values ranged from 25 to 43 mm over all experiments. The fact that such values were consistently larger than the flow separator channel width, $\Delta h = 12.7$ mm, implies that the initial growth of lengthscales was faster than that in the self-similar region. In previous USF studies, the extrapolated values of the measured integral lengthscales ranged from roughly 50% to 80% of the flow separator channel width. Typical estimates of the above integral lengthscales, evaluated at a reference position in the self-similar region of each flow (identified by the corresponding total strain, τ_s), and presented in table 1, ranged from 30% to 52% of the test section height. These results need not be disconcerting because it is well known (Tavoularis & Corrsin 1981) that transverse lengthscales are but a fraction of $L_{11,1}$ (e.g. $L_{11,2} \approx 0.33L_{11,1}, L_{22,1} \approx 0.23L_{11,1}, L_{33,1} \approx 0.34L_{11,1}$).

The streamwise Taylor microscale, λ_{11}, was estimated from the quasi-isotropic relation

$$\epsilon = B\frac{\nu q^2}{\lambda^2{}_{11}} \tag{3.3}$$

where the coefficient B was estimated by the average value of 12 (over previous USF data), rather than the isotropic value of 15. These estimates of λ_{11}, together with the corresponding estimates of the turbulence Reynolds number, $R_{\lambda 1} = u'_1\lambda_{11}/\nu$, at the reference positions are also shown in table 1. The latter was typically 1100 over the range of the present measurements, which is approximately four times larger than the largest values reported in USFs at lower shear rates (TK).

Finally, the Kolmogorov microscale was estimated using its definition, $\eta = (\nu/\epsilon)^{1/4}$. In the present experiments, $\eta/L_{11,1}$ was typically about 4.5×10^{-4}, which is an order of magnitude smaller than values at lower shear rates.

In conclusion, the turbulence in the present experiments was much more energetic and had a much finer structure than that at lower shear rates.

4. Analysis and discussion of the results

4.1. *Measures of mean shear strength*

For a meaningful comparison of different shear flows, one would require a measure of mean shear that is preferably dimensionless and which can be defined unambiguously in USF in wind tunnels, DNS and turbulent boundary layers. If possible, this measure should also be adjustable by external means, independently of the turbulence, which could be viewed as a dependent property. In the absence of a quantity that satisfies all these requirements, we shall identify and discuss a number of other parameters that appear to be suitable for certain types of comparisons.

In an unbounded USF, the sole externally imposed parameter is the value of the mean shear, which coincides with both the mean vorticity and the mean strain rate. Its inverse, $t_s = (\mathrm{d}\overline{U}_1/\mathrm{d}x_2)^{-1}$, constitutes the timescale of mean shear, which can also be viewed as the characteristic 'straining' time. Clearly and undoubtedly, any measure of shear strength should contain t_s. The magnitude of this parameter would be appropriate for comparing USFs generated in the same facility (e.g. by fixing the channel height, Δh, in the flow separator, which fixes the initial dominant eddy size) and at the same wind tunnel speed. On the other hand, it is known (see §3.2) that t_s is proportional to the wind tunnel mean speed and that the Reynolds stresses scale with that speed, which make t_s inappropriate even for comparing flows in the same facility but at different mean speeds. Furthermore, t_s cannot be used for comparisons with turbulent boundary layers, where it depends strongly on distance from the wall, streamwise position and Reynolds number.

A parameter that contains both the mean speed and the shear rate is the flow generator constant, k_s, which, nevertheless, has the dimension of an inverse length and so it does not meet the non-dimensionality requirement. Again, k_s would be a meaningful measure of shear only for comparing USFs in the same facility, although the requirement of matching the mean speed can now be relaxed, within a moderate range. Additional limitations of this quantity are that it is not Galilean invariant and it cannot be defined in a DNS, where there is no mean convection speed, and in boundary layers, where it varies from zero (in the free stream) to infinity (at the wall).

Non-dimensionalization of k_s could be achieved with the use of another lengthscale. In turbulent boundary layers, the obvious external lengthscale would be the distance from the wall, y. It is quite interesting to note that the dimensionless shear rate $k_s y$ is constant both within the viscous sublayer, where it is 1.0, and within the outer layer, where, if one assumes a power law with an exponent $1/n$, it is equal to $1/n$, or about 0.145 for plane boundary layers. This difference is consistent with the expectation that shearing effects should be much stronger closer to the wall. The constancy of the two values within the corresponding regions is also compatible with the hypothesis of two distinct types of turbulence structures and not of a continuously varying one. On the other hand, an external lengthscale cannot be defined in USF, away from its origin and the wind tunnel walls. A design parameter for the type of experimental apparatus used here is the channel height, Δh, of the flow separator, which represents an initial lengthscale but could be very different from the average eddy size far away from the origin. The range of the product $k_s \Delta h$ in the present experiments (0.15 to 0.25) overlapped with the range of the low-shear USF (0.12 in the Tavoularis and Corrsin (1981) experiments and 0.17 in the TK experiments). A more appropriate local dimensionless length would be $k_s L_{11,1}$, but this parameter grows downstream at a rate depending on the mean shear. It may be worth noting that typical values of this

parameter in the present experiments were about 0.8, roughly three to four times larger than those in low-shear USF. One cannot fail but notice a correspondence between the numerical values of the parameter $k_s L_{11,1}$ in low-shear/high-shear USF and of $k_s y$ in outer/inner boundary layers. Although there is a physical connection between eddy size and distance from the wall, this correspondence may be simply fortuitous. Both of these parameters can be viewed as the ratio of the mean velocity difference across an energy-containing eddy and the average convection velocity, which, in an unbounded flow, should not have an effect on the turbulence structure. Large values of these parameters may also indicate an increasing transverse inhomogeneity and an increasing inappropriateness of the centreline velocity to describe the convection of all eddies. Finally, a comparable parameter cannot be defined in the DNS studies, which have no mean convection.

The above discussion leaves only one possible avenue: to non-dimensionalize the mean shear by a turbulent scale, if possible one that does not change rapidly across or along the flow. The turbulent activity, at least the one represented by the most energetic motions, is customarily represented by the 'eddy lifetime' (also known as 'eddy turnover time'), $t_u = q^2/\epsilon$. In flows where the mean shear is the dominant source of turbulent kinetic energy, a natural scale for non-dimensionalizing t_s would be t_u. The ratio t_u/t_s may be viewed as the relative lifetime of an energetic eddy per unit time required for its generation. Obviously, in a self-preserving flow, the faster the eddies are generated, the faster they would be dissipated as well. Nevertheless, the value of the ratio t_u/t_s may depend on the strength of shear, as this may affect the turbulence structure and the mechanisms of production and dissipation. In this sense, this ratio, although a dependent variable, may also serve as an indicator of the strength of shear. For convenience, this ratio may also be expressed in the following form:

$$\frac{t_u}{t_s} = \frac{q^2}{\epsilon}\frac{\mathrm{d}\overline{U}_1}{\mathrm{d}x_2} = \frac{1}{-m_{12}(\epsilon/P)} \tag{4.1}$$

where $P = -\overline{u_1 u_2}\mathrm{d}\overline{U}_1/\mathrm{d}x_2$ is the energy production. The latter form exposes the two factors that determine the ratio t_u/t_s, namely the turbulence structure, via m_{12}, and the dissipation to production ratio, ϵ/P. It is the value of the ratio t_u/t_s that has been used as a measure of shear strength in DNS, denoted by S^*; in some studies, it is twice this ratio that has been used, denoted by Sk/ϵ.

4.2. *Comparisons with previous USF, turbulent boundary layers and DNS*

The first issue to resolve is whether the present flows can be considered as strongly sheared, compared to previous USF realizations in wind tunnels. Estimates of various parameters containing the mean shear are presented in table 1, which shows that the presently achieved values of t_s were an order of magnitude larger than those achieved in previous USF, while the present values of k_s and $k_s L_{11,1}$ were about three to four times larger. Considering the similarity of design of the different facilities, these observations may be interpreted as an indication of 'high shear'. On the other hand, such evidence could be contested by devising a hypothetical pair of flows with identical structures but differing values of these parameters, for example by convecting the entire flow field at different speeds. The 'high shear' claim seems, however, to be justifiable by the additional fact that the t_u/t_s achieved here were, as a whole, measurably larger than previous USF values.

Before further comparisons, it seems necessary to summarize the relevant boundary layer and DNS results. The boundary layer measurements of Laufer (1954),

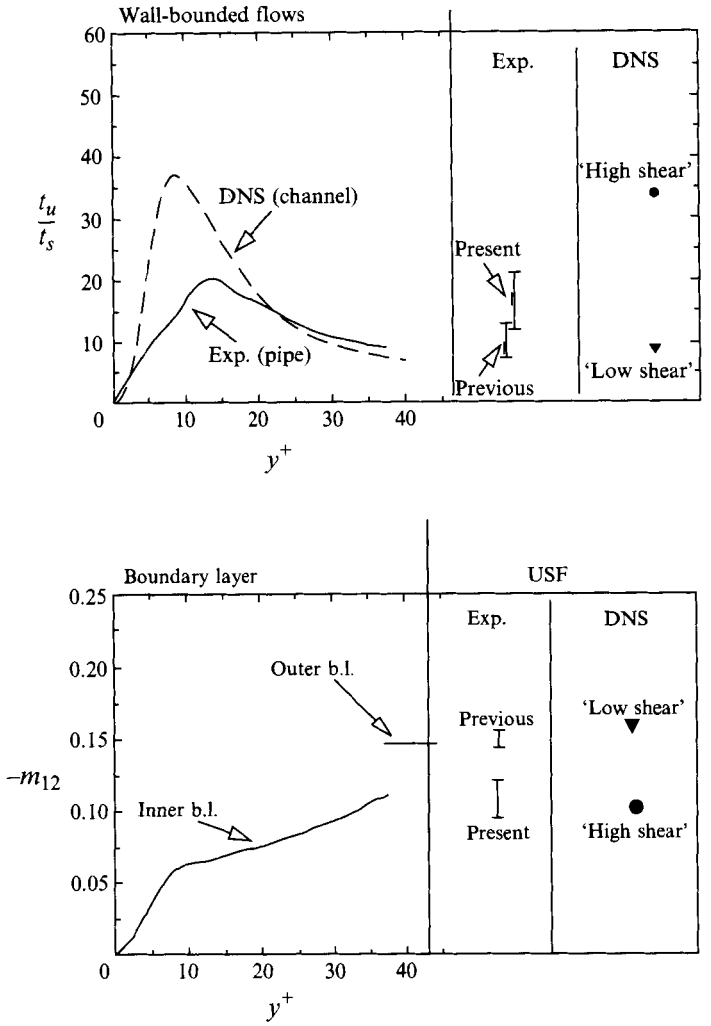

FIGURE 4. Variation of the parameters t_u/t_s and $-m_{12}$ in the present and previous flows.

Eckelmann (1974) and Chevrin, Petrie & Deutsch (1992) and the DNS of USF by Rogers & Moin (1987) and Lee *et al.* (1990) and of channel flow by Kim, Moin & Moser (1987) will be used as representative. The ratio ϵ/P in the boundary layer was estimated from energy balance measurements reported by Laufer (1954). Figure 4 plots the variations of t_u/t_s and m_{12} *vs.* the dimensionless distance y^+ from the wall in the inner boundary layer and the channel flow DNS. Values of these parameters in the various USFs have also been inserted in the figure. In the wall-bounded flows, whereas k_s decreases monotonically from ∞ at the wall to 0 in the free stream, t_u/t_s increases from 0 at the wall (notice that, at the wall, $q^2 \to 0$, while $\epsilon \neq 0$) to a maximum around $y^+ = 10$ to 12, and then it decreases asymptotically to values near 9 in the outer half of the logarithmic sublayer and beyond. A point to be noticed here is that the maximum t_u/t_s in the channel flow DNS was about 36, almost twice as large as the corresponding value in the boundary layer. The shear stress anisotropy magnitude decreases monotonically from about 0.15 in the outer layer to 0 at the wall. At this point it would be instructive to recall that, in the inner boundary layer,

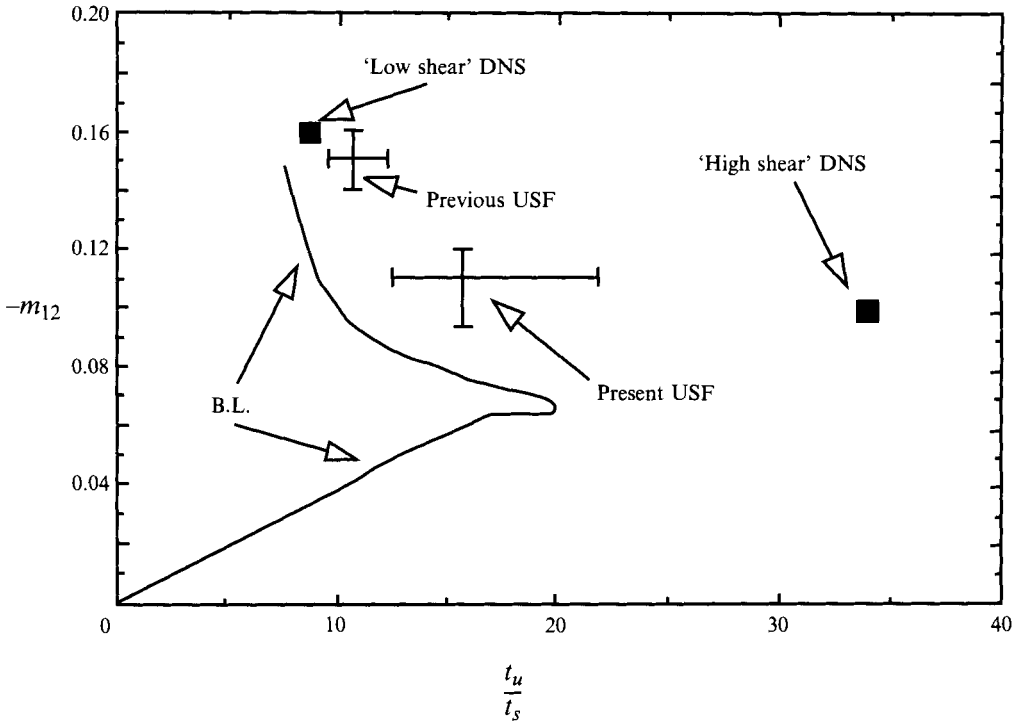

FIGURE 5. Variation of the shear stress anisotropy with the ratio t_u/t_s in the present and previous flows.

transverse motions are hindered by the wall; as a result, the transverse fluctuations vanish at the wall ($m_{22} \to -0.33$), while most of the residual turbulent kinetic energy is carried by the streamwise component ($m_{11} \to 0.50$). The magnitude of the shear stress correlation coefficient, ρ, was found to decrease from about 0.50 in the outer layer to about 0.35 in the buffer sublayer and then it appears to increase again towards 0.50; however, estimates of ρ in the viscous sublayer are less reliable than those of m_{12} because of the dramatically decreasing transverse velocity, which appears in the denominator of ρ.

A comparison of the wind tunnel USF data and the boundary layer data presented above clearly shows that the general trends in the values of t_u/t_s, m_{12} and ρ in USF with increasing mean shear are similar to the trends of these parameters across the boundary layer, as the inner sublayer (nominally the range $20 < y^+ < 40$) is approached from the outer layer. The DNS results also agree qualitatively with the above trends. The quantitative difference between the 'high shear' DNS estimates of t_u/t_s and the corresponding boundary layer measurements can be attributed to the fact that the shear rate in the DNS of Lee *et al.* (1990) was adjusted to match the conditions near the peak t_u/t_s in the channel flow DNS, which was substantially higher than that in a moderate Reynolds number boundary layer.

Finally, in an effort to establish a possible relationship between the anisotropy and the relative shear strength, measurements of $-m_{12}$ for USF and boundary layers were plotted versus t_u/t_s in figure 5. Although the trends indicated by all data were the same, $-m_{12}$ values in USF were consistently 30% to 40% higher than the corresponding values in boundary layers for the same t_u/t_s, thus precluding the fitting of a universal empirical curve.

The above discussion has clearly demonstrated a decrease in the shear stress anisotropy with increasing shear in all shear flows considered. The normal stress anisotropies, although showing similar trends in the boundary layer and the DNS flows, had no systematic trend in the USF. This difference may be attributed to two effects. Firstly, it is possible that the shear in the present USF may be strong enough to influence m_{12}, which, in general, is the most sensitive indicator of the turbulence structure (see, for example, its sensitivity to streamline curvature, discussed by Holloway & Tavoularis 1992), but not the normal anisotropies; one may note that the DNS that contain an effect on the normal anisotropies were performed at substantially higher shear rates. Secondly, it is quite possible that a free shear flow cannot reproduce the changes in the partition of turbulent kinetic energy occurring near a wall and which are primarily due to its kinematic constraint.

5. Concluding remarks

Nearly homogeneous USFs have been generated at shear rates higher than ever before, in an attempt to simulate shearing conditions in the inner boundary layer. The measurements show that the turbulence structure attains a self-similar state with approximately constant dimensionless stresses and exponential kinetic energy growth, in agreement with USF at lower shear rates. The main difference from realizations at lower shear rates was a marked (about 25%) decrease in the turbulent shear stress anisotropy. It would be interesting to investigate whether this quantity would further decrease at even higher shear rates. Unfortunately, preliminary considerations indicate that a substantial further increase in the shear rate of a USF generated in a wind tunnel may not be possible without introducing compressibility effects (Sarkar, Erlebacher & Hussaini 1991; Blaisdell, Mansour & Reynolds 1993) on the high-speed side of the flow. Ideally, the maximum value of k_s achievable in a wind tunnel is $2/h$, where h is the test section's height. The present value of $h = 127$ mm is probably as small as one could use without severely compromising the transverse homogeneity of the flow and the spatial resolution of the measuring techniques.

The present measurements are compatible with the hypothesis that the high rate of mean shear (or mean deformation), and not necessarily the damping of normal velocity fluctuations due to the presence of a solid boundary, may be responsible for the greater relative suppression of Reynolds shear stress compared to the turbulent kinetic energy change.

The support of Dr L. Chan, Head, and the assistance of the staff of the High Speed Aerodynamics Laboratory of the National Research Council of Canada are highly appreciated. Particular thanks are due to Mr S. Pynn for his help with the measurements. We are also grateful to a referee for a constructive review. Financial support for this project was provided by the Natural Sciences and Engineering Research Council of Canada.

REFERENCES

BLAISDELL, G. A., MANSOUR, N. N. & REYNOLDS, W. C. 1993 Compressibility effects on the growth and structure of homogeneous turbulent shear flow. *J. Fluid Mech.* **256**, 443–485.

BRERETON, G. L. & HWANG, J.-L. 1994 The spacing of streaks in unsteady turbulent wall-bounded flow. *Phys. Fluids* **6**, 2446–2454.

CHEVRIN, P.-A., PETRIE, H. L., & DEUTSCH, S. 1992 The structure of Reynolds stress in the near-wall region of a fully developed turbulent pipe flow. *Exps. Fluids* **13**, 405–413.

ECKELMANN, H. 1974 The structure of the viscous sublayer and the adjacent wall region in a turbulent channel flow. *J. Fluid Mech.* **65**, 439–459.

HOLLOWAY, A. G. L. & TAVOULARIS, S. 1992 The effects of curvature on sheared turbulence. *J. Fluid Mech.* **237**, 569–603.

KIM, J., MOIN, P. & MOSER, R. 1987 Turbulence statistics in fully developed channel flow at low Reynolds number. *J. Fluid Mech.* **177**, 133–166.

LAUFER, J. 1954 The structure of turbulence in fully developed pipe flow. *NACA Tech. Rep.* 1174.

LEE, M. J., KIM, J. & MOIN, P. 1990 Structure of turbulence at high shear rate. *J. Fluid Mech.* **216**, 561–583.

ROGERS, M. M. & MOIN, P. 1987 The structure of the vorticity field in homogeneous turbulent flows. *J. Fluid Mech.* **176**, 33–66.

ROHR, J. J., ITSWEIRE, E. C., HELLAND, K. N. & VAN ATTA, C. W. 1988 An investigation of the growth of turbulence in a uniform mean-shear-flow. *J. Fluid Mech.* **187**, 1–33.

SARKAR, S., ERLEBACHER, G. & HUSSAINI, M. Y. 1992 Compressible homogeneous shear: simulation and modeling. In *Turbulent Shear Flows* (ed. F. Durst *et al.*), vol. 8, pp. 249–267. Springer.

SOUZA, F. A. DE 1993 Experiments in highly sheared, nearly homogeneous turbulence. M.A.Sc. thesis, University of Ottawa.

TAVOULARIS, S. 1985 Asymptotic laws for transversely homogeneous turbulent shear flow. *Phys. Fluids* **28**, 999–1001.

TAVOULARIS, S. & CORRSIN, S. 1981 Experiments in nearly homogeneous turbulent shear flow with a uniform mean temperature gradient. Part 1. *J. Fluid Mech.* **104**, 311–347.

TAVOULARIS, S. & KARNIK, U. 1989 Further experiments on the evolution of turbulent stresses and scales in uniformly sheared turbulence. *J. Fluid Mech.* **204**, 457–478 (referred to herin as TK).